

Chitin Filaments from Dibutrylchitin Precursor: Fine Structure and Physical and Physicochemical Properties

G. URBANCZYK,¹ B. LIPP-SYMONOWICZ,¹ I. SZOSLAND,² A. JEZIORNY,¹ W. URBANIAK-DOMAGALA,¹ K. DORAU,¹ H. WRZOSEK,¹ S. SZTAJNOWSKI,¹ S. KOWALSKA,¹ E. SZTAJNERT¹

¹ Institute of Fiber Physics and Textile Finishing, Technical University of Lodz, 36 Zwirki Street, 90–924 Lodz, Poland

² Department of Physical Chemistry of Polymers, Technical University of Lodz, Poland

Received 15 July 1996; accepted 5 December 1996

ABSTRACT: Chitin filaments obtained after alkaline hydrolysis of dibutrylchitin (DBCH) precursor filaments were investigated. The morphological structure, fine structure, and selected physical and physicochemical properties were studied. The studies of morphological structure included the assessment of the cross-section profile, the length and developing index of the contour line of the cross sections, the appearance of spherulitical crystalline aggregations, and the existence of skin–core building. The appraisal of the fine structure comprised the recognition of the lattice crystal system and the parameters of the unit cell, the crystallinity degree and average lateral crystallite sizes, and the crystalline and amorphous orientation. The characterization of physical properties included the appraisal of density, mechanical, thermal, electrical, and optical properties. In the area of physicochemical properties, swelling and dyeability were examined. © 1997 John Wiley & Sons, Inc. *J Appl Polym Sci* **65**: 807–819, 1997

Key words: chitin; filament; structure; properties

INTRODUCTION

Chitin, a natural polymer present very widely and abundantly in nature, is an essential supporting structure for several living organisms—animals as well as plants. In the case of the first (arthropods, invertebrates, insects, molluscs, and annelids), chitin is an alternative for protein, especially for collagen, and exists together with it, as the cuticulae or skeleton part of the animal.

In the case of plants (fungi, algae, and spines of eurytholine diatoms), chitin is an alternative for cellulose, and occurs together with it as cell wall material or extracellular spines.

Chitin is a linear polysaccharide composed of 1,4-linked *N*-acetyl-D-glucosamine residues (NGA), exhibiting along the chain a repeat unit of 10.3 Å length.

Chitin, as has been confirmed by numerous investigations, reveals excellent biological properties (bioactivity and biocompatibility), making it a valuable polymeric material that can be utilized for biomedical purposes.

A major drawback to its utilization is the intractability.

Chitin is very hardly soluble. It can be dissolved only in a few compounds such as inorganic acids, highly concentrated formic acid, and DMA–LiCl. Its poor solubility is a result of the close packing of chains and its strong inter- and intramolecular bonds of four different types¹ among the hydroxyl and acetamide groups. The very poor solubility excludes on principal the formation of fibers. Few attempts to produce fibers from commenced by Kunike² and later on by Tokura³ can be regarded as little promising. In the presented contribution we are reporting about chitin filaments obtained from a chemical conversion of the precursor dibutryl-

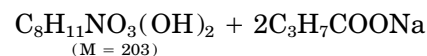
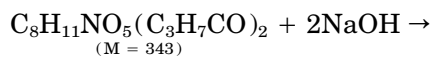
Correspondence to: G. Urbanczyk.

© 1997 John Wiley & Sons, Inc. CCC 0021-8995/97/040807-13

Table I Chitin Content After Alkaline Hydrolysis of DBCH Filaments Ascertained on the Base of Elementary Analysis for Nitrogen

Order Number	Reaction Time (min)	Contents <i>N</i> (%)	Chitin Contents (mol %)	Hydrolysis Terms
1	0	4.08	0	Excess of 1.25 <i>M</i> NaOH; temp. 25°C; DBCH with $\langle\eta\rangle = 1.28$
2	60	5.31	56.0	
3	90	5.69	70.0	
4	150	6.14	83.0	
5	360	6.37	97.0	

chitin (DBCH) filaments. The performed analysis gives evidence that the filaments examined consist almost totally of purified chitin.



EXPERIMENTAL

Materials

The chitin filaments investigated were obtained by alkaline hydrolysis of precursor DBCH filaments. The utilized DBCH filaments were spun from 22% acetone solution of polymer with intrinsic viscosity $\langle\eta\rangle = 1.28$, using a dry method of spinning.⁴ The average thickness of the filaments was ca. 40 μm .

The hydrolysis was conducted in the following manner: water solution of NaOH with concentrations of 0.939*M* and 1.25*M* were used as a hydrolysis medium. Hydrolysis reaction was carried out at 25°C. Weighed samples of DBCH filaments in loose state were put in excess of NaOH solution for a definite period, then they were taken out, washed to remove any trace of alkali, dried, and weighed again. The scheme of hydrolysis reaction is as follows:

The efficiency of chitin reconversion was checked threefold, by means of IR spectroscopy, analyzing the disappearance of 1740 cm^{-1} absorption bands referring to ester bonds in DBCH filaments; by means of elementary analysis of the increase of nitrogen contents after the hydrolysis; and by ascertaining the weight losses of DBCH filaments after the hydrolysis. As evidence of the alkaline hydrolysis efficiency dates referring to the chitin content and to the diminishing of 1740 cm^{-1} absorption bands in DBCH are presented in Tables I and II and Figure 1. For study, filaments with a contents of chitin above 92% were chosen.

Testing Procedures

The morphological structure of the filaments was examined qualitatively as well as quantitatively. The shape of cross-sections, their contour line length and developing index, the mean value of the cross-sectional surfaces along with the appraisal of the presence of skin–core structure and

Table II Chitin Content After Alkaline Hydrolysis of DBCH Filaments Ascertained on the Base of the Weighing Method

Order Number	Reaction Time (min)	Weight Loss (%)	Chitin Contents (mol %)	Concentration of NaOH (<i>M</i>)	Temp (°C)
1	60	21.3	52.2	1.25	25
2	90	28.9	70.8		
3	150	36.4	89.2		
4	240	37.7	92.4		
1	60	15.8	38.7	0.938	25
2	90	24.4	59.8		
3	150	34.4	84.3		
4	420	40.5	99.2		

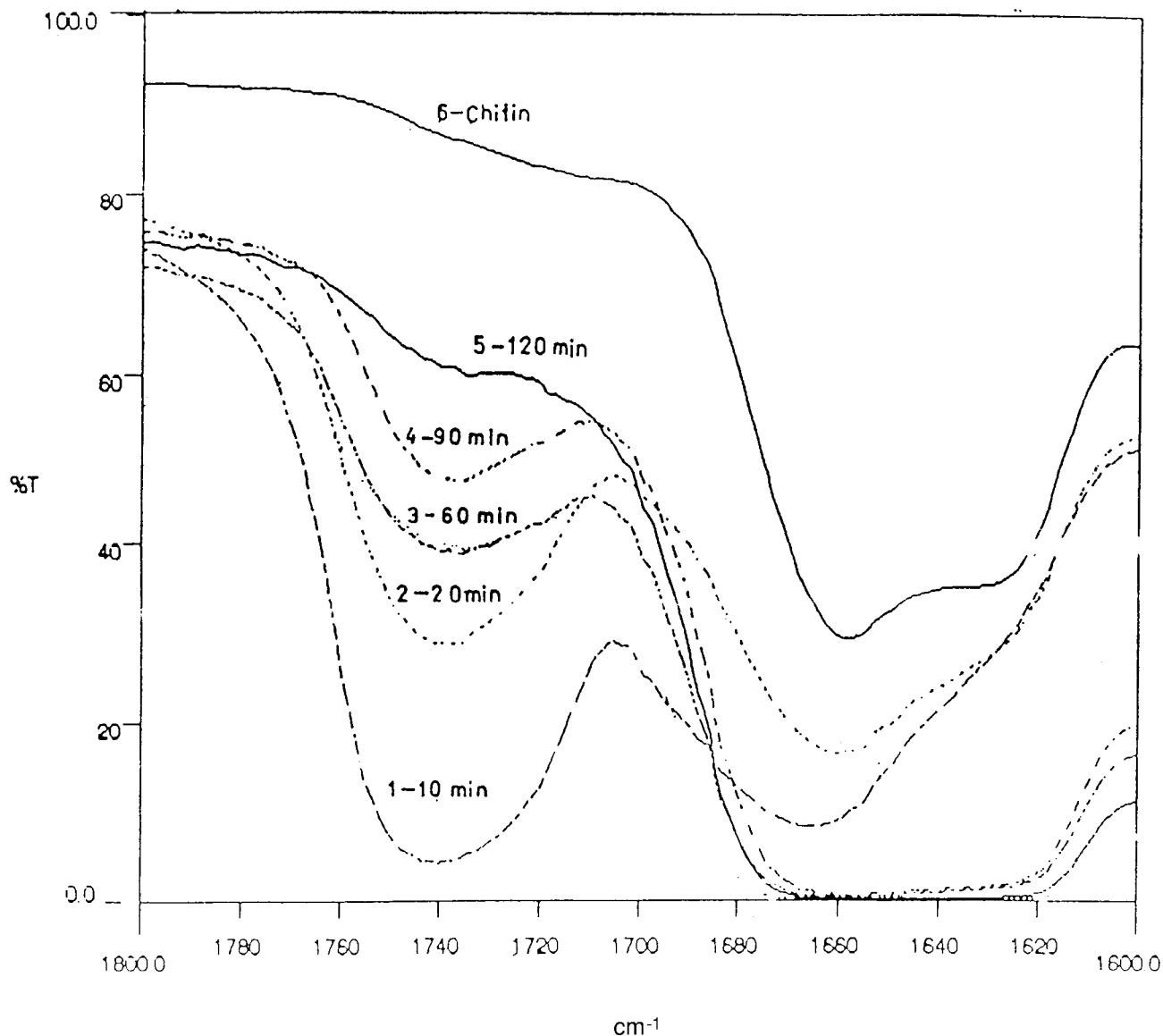


Figure 1 Disappearance of 1740 cm^{-1} IR absorption band correlated with the ester groups, as a result of alkaline hydrolysis of DBCH.⁴

occurrence of spherulitical crystalline aggregates were examined. The first kind of measurements were carried out using optical microscopy at a magnification of $600\times$ involving a computer image analyzer IMAL. The second type of examination was based on polarization interference microscopical observations by the application of the differential homogenous interference field of 0 and 1 order. These observations were carried out on the BIOLAR-PI microscope in monochromatic light of $\lambda = 0.589\ \mu\text{m}$ at magnitude of 12.5×20 .

The recognition of the kind of crystalline structure, the evaluation of the crystallinity degree, and the assessment of the average lateral crystallite size was founded on WAXS investigations

carried out on a DRON-3 diffractometer at the following operating parameters: $\text{CuK}\alpha$, 15 mA and 40 kV, and slit $0.5 \times 0.5\ \text{mm}$. The X-ray evaluation of the degree of crystallinity was performed on the basis of measured integral diffracted intensities of chitin samples and the standard reference sample (cellulose I) of known crystallinity degree, by regarding the differences in X-ray scattering ability of both kinds of specimens, according to the procedure of Hermans and Weidinger.⁵

The degree of crystallinity has been additionally determined by means of the densitometric method. The degree of crystallinity was then calculated from the known formula

$$X = d_{\text{cr}}/d_s((d_s - d_{\text{amph.}})/(d_{\text{cr}} - d_{\text{amph.}}))$$

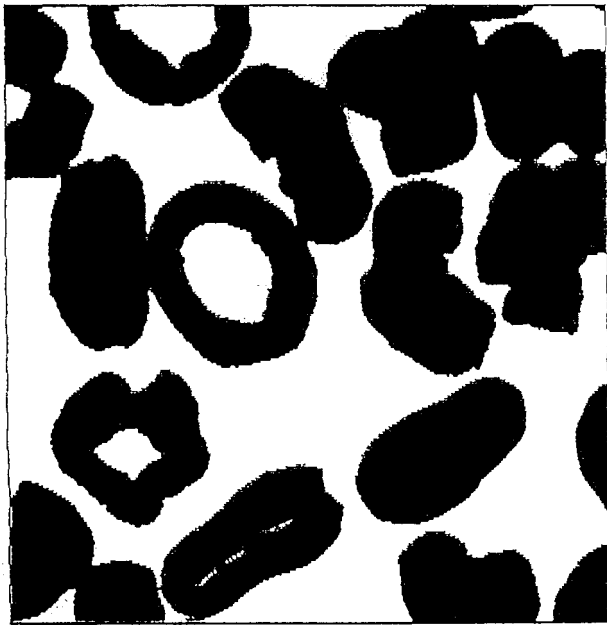


Figure 2 Cross sections of DBCH filaments.

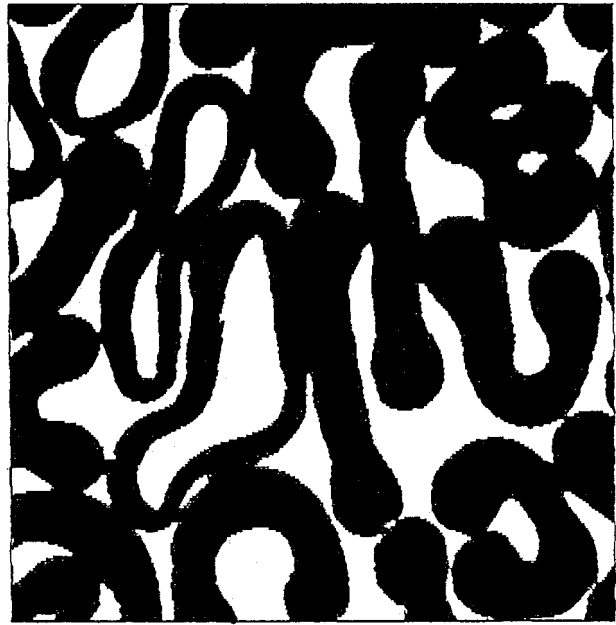


Figure 3 Cross sections of chitin filaments.

on the basis of the measured sample density d_s and the theoretical values of the crystalline d_{cr} and amorphous $d_{amph.}$ densities of chitin established by the authors. The sample density was measured using the gradient column technique in the mixture of toluene and CCl_4 at $20^\circ C$. The value of d_{cr} was calculated on the basis of the assumed lattice unit cell and is equal to 1.4936 g/cm^3 . The theoretical amorphous density $d_{amph.}$ was computed from the formula

$$d_{amph.} = K \times M/N \times \Sigma \Delta V_i$$

where K is the coefficient of molecular packing of the amorphous phase, N the Avogadro constant, M the molecular weight of the chain repeat unit $M = 203$, $\Sigma \Delta V_i$ the Van der Waals increments of

the constituent groups $\Sigma \Delta V_i = 169.5 (\text{\AA}^3)$. In the situation having no information about the packing coefficient K for amorphous chitin, an attempt was made to estimate it in indirect manner. Taking into consideration the chemical resemblance between chitin and acetatcellulose, the sought K value was calculated as a corrected K value for amorphous acetatcellulose. The correction consisted of regarding the differences in size of the side groups of both polymers. The approximate value of K thus calculated is $K = 0.666$.

The value of the theoretical amorphous density of chitin computed from the above formula is equal to $d_{amph.} = 1.3250 (\text{g/cm}^3)$.

The average lateral crystallite sizes D_{010} and D_{100} were calculated on the basis of the measured 010 and 100 diffraction peaks of the WAXS

Table III Parameters of the Chitin Lattice Unit Cells

Polymorphic Form	Unit Cell Parameters				Cell Volume (\AA^3)	Number of NAG Residues on 1 Cell	Density d_{cr} (g/cm^3)	References
	a (\AA)	b (\AA)	c (\AA)	γ (deg)				
α -Modyfic	4.76	18.85	10.28	90°	922.38	4	1.461	9
	4.74	18.86	10.32	90°	922.57	4	1.461	10
β -Modyfic	4.70	10.50	10.30	$\approx 90^\circ$	508.30	2	1.3260	11
	4.80	9.83	10.32	112°	451.39	2	1.4130	12
	4.85	9.26	10.38	97.5°	462.32	2	1.4580	13-15
γ -Modyfic	4.57	9.60	10.30	90°	451.90	2	1.4919	16
	8.90	17.0	10.25	90°	1550.82	6	1.304	17

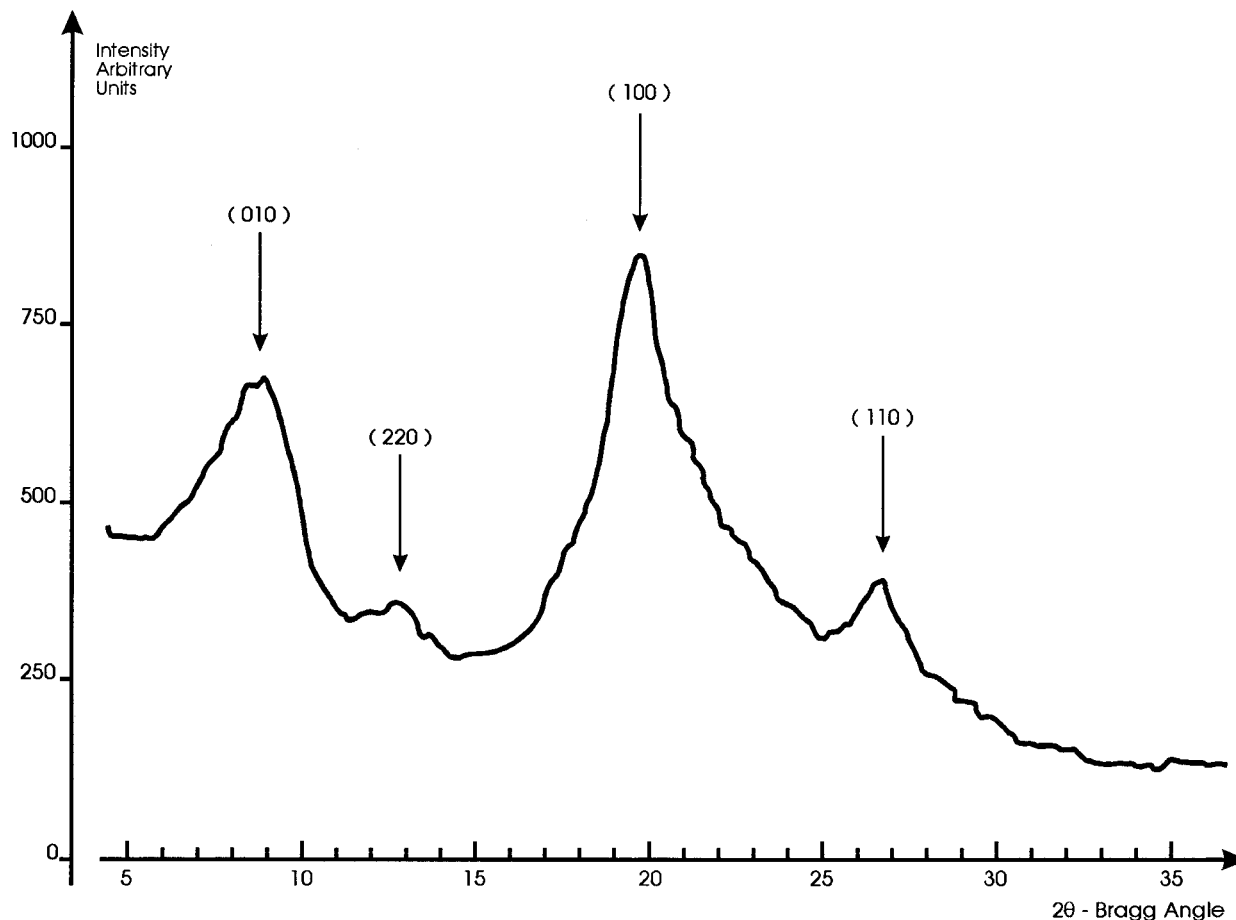


Figure 4 WAXS intensity distribution curve of chitin filaments.

curves. from the fundamental Scherrer expression.⁶

The evaluation of the internal orientation encompassed the crystalline and the amorphous orientation. The crystalline orientation was appraised on the basis of the azimuthal intensity distribution $I(\delta)$ within the equatorial 010 and 100 reflections. For the known intensity distribution $I(\delta)$ and known $2\theta_{010}$ and $2\theta_{100}$ there were calculated values $\langle \cos^2 \rho_{010} \rangle$ and $\langle \cos^2 \rho_{100} \rangle$, where

ρ is the polar angle of corresponding lattice planes. Further, the crystallite orientation factor $\langle \cos^2 \phi \rangle$ was computed, where ϕ is the angle between the crystallite axis and the orientation axis of the fiber, from the general formula relevant for monoclinic lattices⁷:

$$\langle \cos^2 \phi \rangle = 1 - \langle \cos^2 \rho_{110} \rangle - 0.5874 \langle \cos^2 \rho_{010} \rangle - 0.4126 \langle \cos^2 \rho_{100} \rangle$$

Finally the Hermans orientation factor was calculated

$$f_c = \frac{1}{2}(3\langle \cos^2 \phi \rangle - 1)$$

Table IV X-ray Diffraction Data of Chitin Filaments

Reflection Intensity	Bragg. Angle 2θ (degree)	Interplanar Spacing d_{hkl} (Å)	Miller Indices (hkl)
Strong	8.8-9.0	9.11	(010)
Weak	12.5-12.8	7.00	(220)
Very Strong	19.5	4.42	(100)
Medium	26.5	3.40	(110)

The amorphous orientation was evaluated on the basis of the IR dichroic ratio $R = D_{\parallel}/D_{\perp}$ and the orientation function f_{IR} calculated from the simplified formula of Fraser⁸ $f_{IR} = (D_{\parallel} - D_{\perp})/(D_{\parallel} + 2D_{\perp})$ of the so-called "amorphous" bands. There were considered dichroitic bands correlated with

Table V Degree of Crystallinity and Average Lateral Crystallite Sizes

Kind of Filament	Degree of Crystallinity		Lateral Crystallite Size	
	X-ray	Densitometric	D_{100} (Å)	D_{010} (Å)
DBCH Precursor	0.13	0.23	18.2	54.5
Chitin	0.26	0.33	27.0	55.5

—CH₃ groups (1455 cm⁻¹ and 1375 cm⁻¹) present in spectra of chitin as well as of DBCH filaments. The dichroic ratio evaluation was performed on spectrograms obtained from the SHIMADZU FT-IR spectrophotometer 8101M at the following operating parameters: measuring mode A, resolution 4.0–8.0 cm⁻¹ accumulation 40 and 200, detector 2.8 cm/s and Happ-Genzel apodization.

The investigations into the mechanical properties comprised appraisal of tensile strength σ , elongation at rupture ε , and the initial modulus E . The results were obtained from stress-strain curves measured on the 1111 INSTRON table universal instrument at operating parameters of 20°C, 20% and 65% RH, 5 mm/min extension rate and 10 mm gauge length. The reported values are averages of 40 independent measurements.

The thermal properties were examined by means of differential scanning calorimetry (DSC) using the Du Pont 990 thermoanalyzer at operating parameters of nitrogen atmosphere, heating rate of 10°/min, and calorimetric sensitivity of 1 mcJ/s.

The electrical properties of filaments were evaluated on the basis of assigned values of volume resistivity ρ . The sought volume resistivity was calculated from the formula

$$\rho = R_v \times m/d \times l^2 \quad (\Omega \times m)$$

where R_v is the average electrical resistance of

the sample of parallelized filaments (Ω), m is the weight of the sample ($m = 0.01$ g), l is the distance between the electrodes ($l = 1$ cm), d is the density of the filaments (g/cm³).

The values of R_v were established from current intensity-tension characteristics assigned by application of Keithley electrometer type 610 C for the tension range 100–3000 V.

The R_v were calculated from the regression equation $I = f(U)$ as the regression coefficient. The considered R_v are mean values of three independent measurements. The examination was performed on samples conditioned in air of 23°C and RH of 25% and of 23°C and RH of 65%.

The appraisal of physicochemical properties was confined to the assessment of swelling ability in water and solution of physiological salt at 20°C and to the dyeability in different types of dyes.

RESULTS AND DISCUSSION

Morphological Structure

The cross sections of chitin and the precursor DBCH filaments are depicted in Figures 2 and 3. These pictures reveal distinct differences. The chitin, compared to DBCH filaments, exhibit elongated “bone shape” and more regular cross-sections. The average values of the areas of the con-

Table VI Crystalline and Amorphous Orientation Parameters of Chitin and DBCH Filaments

Kind of Filament	Crystalline Orientation				Orient. Plate Effect. $\frac{\langle \cos^2 \rho_{010} \rangle}{\langle \cos^2 \rho_{100} \rangle}$	Amorphous Orientation			
	$\langle \cos^2 \rho_{110} \rangle$	$\langle \cos^2 \rho_{010} \rangle$	$\langle \cos^2 \rho_{100} \rangle$	Hermans Orientation Function f_x		Dichroic Ratio R		Orientation Function F_{IR}	
					1455	1375	1455	1375	
					cm ⁻¹	cm ⁻¹	cm ⁻¹	cm ⁻¹	
DBCH ^a	—	0.2073	0.1911	0.4024	1.085	1.22	1.19	0.067	0.061
Chitin	0.1703	0.2045	0.1796	0.6355	1.138	1.04	1.04	0.0137	0.0130

^a Established after method of the authors (G. Urbańczyk et al.¹⁸).

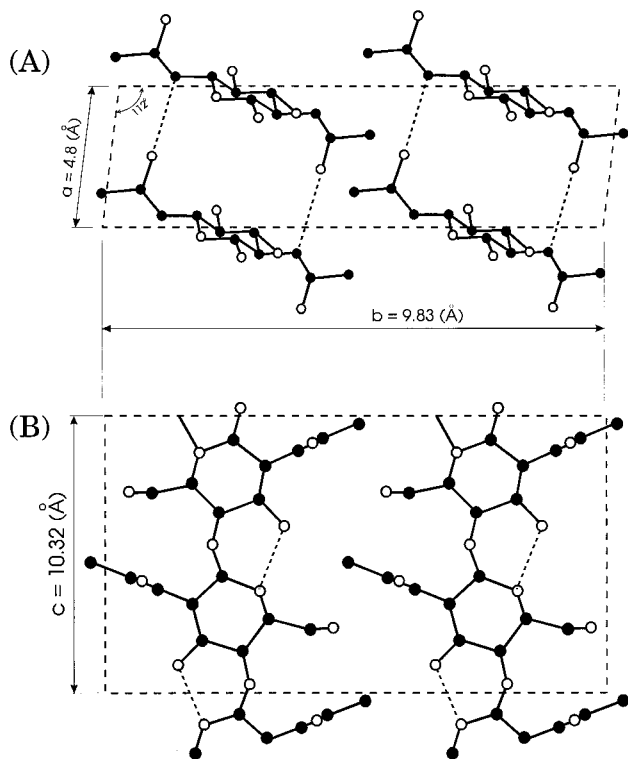


Figure 5 Visualization of the lattice of β chitin in studied filaments. (A) Projection on a-b plane; (B) projection on b-c plane.

four line length and the contour line development indices are correspondingly equal to $1380 \mu\text{m}^2$, $237 \mu\text{m}$, 0.800 for chitin and $1207 \mu\text{m}^2$, $159 \mu\text{m}$, 0.285 for DBCH filaments. These results give evidence that the alkaline hydrolysis of the DBCH precursors causes parallel to the loss of weight an increase of the cross-section surface accompanied by a developing of the cross-section contour line.

The performed investigations give no evidence of the occurrence of skin-core structure for chitin, as well as for DBCH filaments. Examination under polarized light showed no evidence of a spherulitical crystal structure (lack of Maltese cross-brightening patterns) in both kinds of filaments.

Crystalline Structure

Chitin deprived of protein inclusions reveals a strong ability to crystallize. In the natural state, the degree of crystallinity may reach 0.50 – 0.60 . Until now, there have been recognized three polymorphic modifications of crystalline chitin— α , β , and γ . They differ in respect to the crystal system and parameters of the lattice unit cell. These differences are a result of differences in the manner of how adjacent molecules are arranged in the lattice. Chitin chains occurring in the lattice in sheets may be arranged all in a parallel or anti-

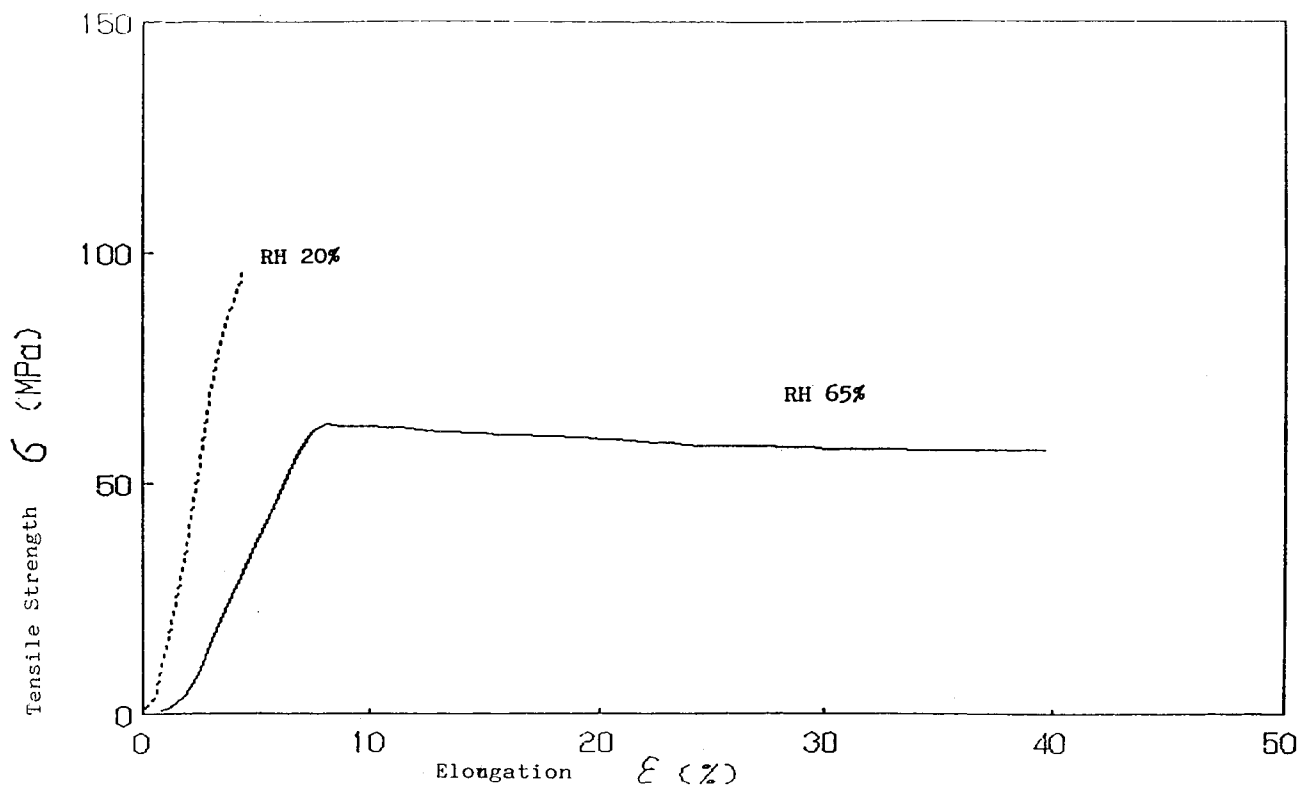


Figure 6 Stress-strain curve of chitin filaments.

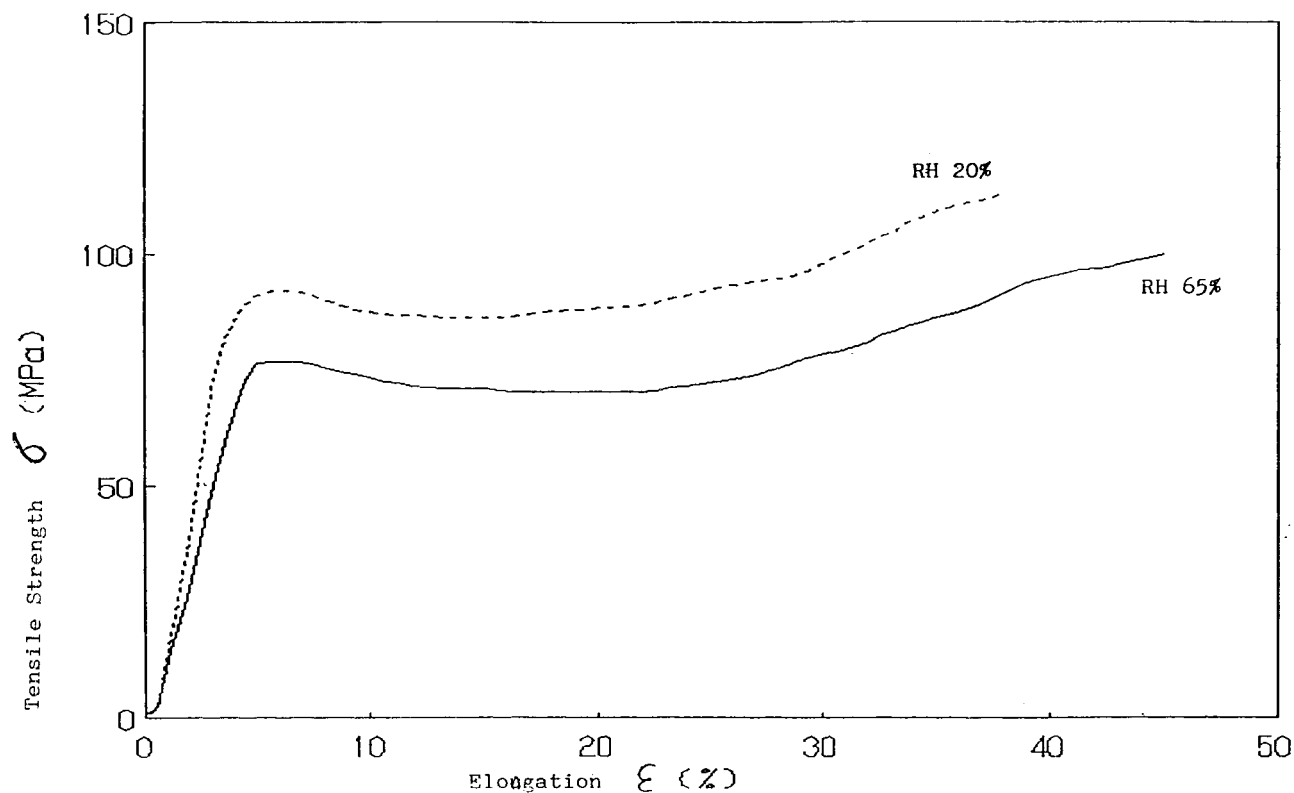


Figure 7 Stress-strain curve of DBCH filaments.

parallel manner: in the case of α -chitin, all antiparallel; in the case of β -chitin, all parallel. The arrangement of chains in the γ -modification is characterized by an alternative appearance of two sheets with parallel arrangement followed by one sheet with antiparallel arrangement. The parameters of lattice unit cells for particular polymorphic crystalline forms of chitin are presented in Table III.

The α polymorphic form is more common than β and γ . It is conspicuous by a strong chemical stability. This is caused by the greatest possible number of inter- as well as intramolecular hydro-

gen bonds. From a point of view of the manner in which the adjacent molecules are arranged in lattice, α chitin reveals resemblance to the cellulose II.

In turn, β -chitin, the second in prevalence, is characterized by a lower stability than the α form. This is due to a minor number of hydrogen bonds, an evidence of lower stability manifests itself in the possibility of transformation of the β into the α form in strong concentrated solution of HCl. The reduced, as compared to the α form, number of hydrogen bonds opens the possibility to permanently link water molecules, which in turn, means

Table VII Mechanical Properties of Chitin and DBCH Filaments

Kind of Filament	Relative Humidity (%)	Rupture Force F (N)	Tensile Strength		Elongation at Rupture		Initial Modulus	
			σ (MPa)	Cv	ε (%)	Cv	E (GPa)	Cv
DBCH	20	0.155	112.4	5.4%	36.2	4.7%	2.6	3.5%
	65	0.135	97.9	6.1%	45.7	3.6%	1.8	2.4%
Chitin	20	0.093	77.1	13.2%	4.6	15.7%	2.2	16.0%
	65	0.070	58.0	2.3%	42.2	13.1%	1.0	9.1%

Cv, coefficient of variation.

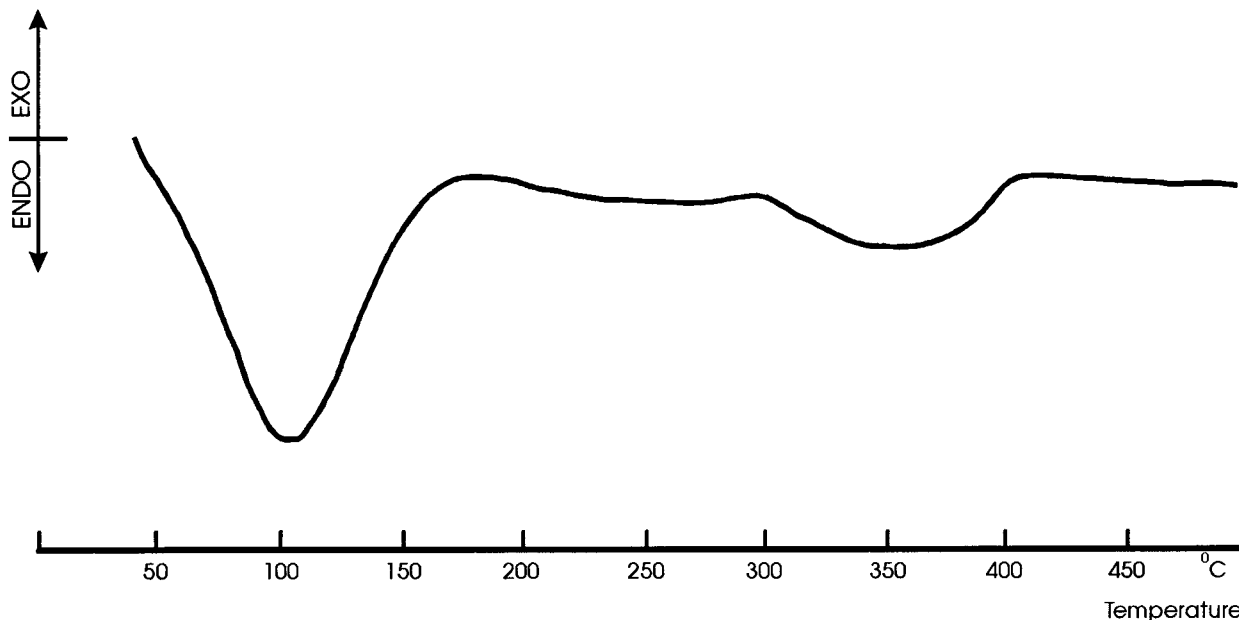


Figure 8 DSC thermogram of chitin filaments.

that chains in the lattice might be regarded as chitin monohydrates. From the point of view of the manner in which chains are arranged in the lattice, β chitin is similar to cellulose I. This resemblance is a reason why Gardner and Blackwell¹⁵ consider the transformation of β into α as analogous to the conversion cellulose I into II. β chitin occurs as a rule in the form of large crystalline fibrils of ribbonlike morphology. The crystal-

line structure of investigated chitin filaments was recognized on the base of X-ray examination. The X-ray diffraction intensity distribution curves obtained exhibit the appearance of four diffraction peaks (Fig. 4). The stated diffraction peaks are in full agreement with the lattice of β crystalline chitin proposed by Dweltz.¹² The reflections ascertained are depicted in Table IV.

The diffraction peaks ascertained give rise to

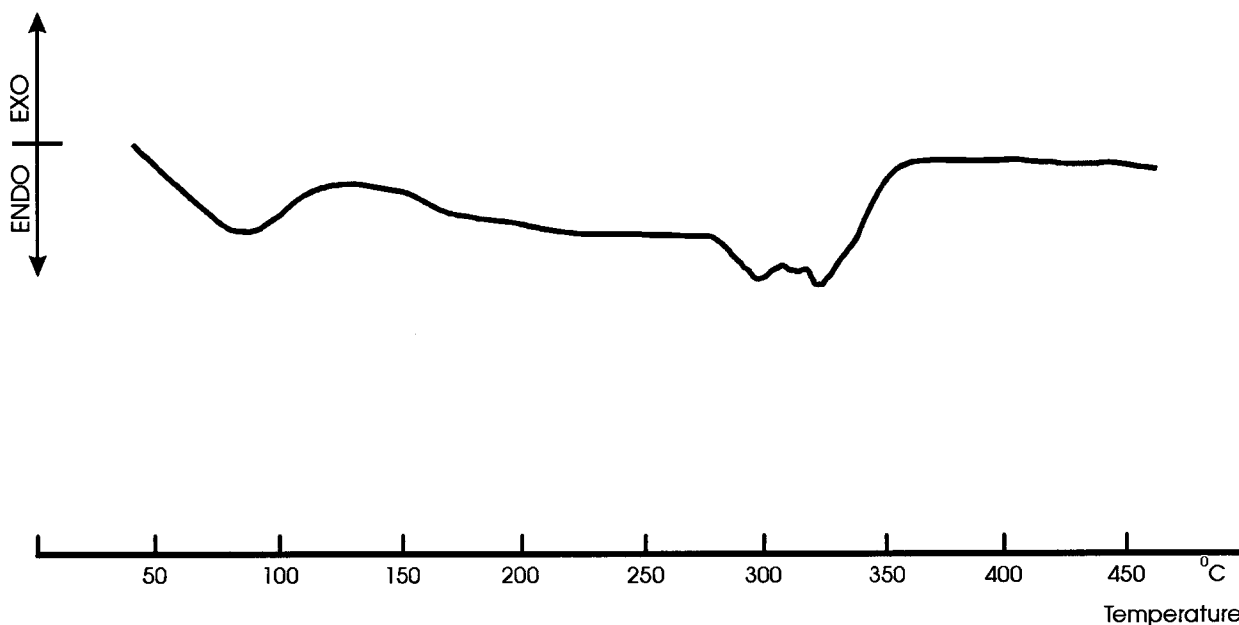


Figure 9 DSC thermogram of DBCH filaments.

Table VIII Electrical Volume Resistivity ρ_v of Chitin and DBCH Filaments

Kind of Filament	Measuring Terms			
	25% RH; $T = 23^\circ\text{C}$	$\delta\rho$	65% RH; $T = 23^\circ\text{C}$	$\delta\rho$
DBCH	$8.1 \times 10^8 (\Omega \text{ m})$	2.0×10^8	$4.6 \times 10^8 (\Omega \text{ m})$	1.2×10^8
Chitin	$1.3 \times 10^8 (\Omega \text{ m})$	0.3×10^8	$4.8 \times 10^7 (\Omega \text{ m})$	0.6×10^7

$\delta\rho$, mean value error of ρ_v .

the assumption that crystalline regions in the investigated chitin filaments represent the β form of crystalline chitin. The lattice is characterized by a monoclinic unit cell with parameters $a = 4.80 (\text{\AA})$, $b = 9.83 (\text{\AA})$, $c = 10.32 (\text{\AA})$, $\gamma = 112^\circ$, determined by Dweltz.¹²

The relatively small number of reflections in the diffraction pattern proves that the lattice is relatively defective, i.e., low perfect in geometrical regularity. The very probable constitution of the lattice is shown in Figure 5.

Crystallinity and Average Lateral Crystallite Sizes

The results of measurements are collected in Table V. It may be inferred from the results that the reconversion of chitin occurring as a result of alkaline hydrolysis of DBCH leads to a noticeable increase in filament crystallinity. One can conclude that this increase proceeds as a result of growth of lateral average crystallite size, especially in the direction perpendicular to the (100) lattice planes.

Additionally, it should be mentioned that the recrystallization proceeding during the alkaline hydrolysis is accompanied by a transformation of the crystalline regions lattice. The lattice of the precursor DBCH filaments, as was ascertained previously by the authors,¹⁸ is characterized by an orthorhombic crystal system with the unit cell $a = 4.4 (\text{\AA})$, $b = 13.4 (\text{\AA})$, $c = 10.3 (\text{\AA})$.

Internal Orientation

The parameters characterizing crystalline and amorphous orientation are presented in Table VI.

Table IX Density and Refractive Index of Chitin and DBCH Filaments

Kind of Filament	Density (g/cm^3)	Refractive Index: $\lambda = 0.589 \mu\text{m}$; 20°C
DBCH	1.2190	1.4928
Chitin	1.3767	1.5283

As one can see, the crystalline orientation of chitin filaments is better, but on the contrary, the amorphous orientation is worse than for the precursor DBCH filaments. It can be assumed that such report of results is a consequence of recrystallization occurring during the alkaline hydrolysis of DBCH. The increase in the amount of crystallized polymer refers first of all to the best-ordered chains of the noncrystalline fraction. The remaining noncrystalline fraction comprises worse-ordered chains. Additionally, the lower amorphous orientation in chitin filaments may also be caused by a very probable disorientation effect occurring in the amorphous phase during the alkaline hydrolysis.

In both kinds of filaments occur a weak but differentiated so-called orientation plate effect. In the case of chitin filaments, the plate effect is more strongly pronounced. This provides indirect information about the morphology of crystallites. From the larger values of the plate effect it may be inferred that in the case of chitin filaments the crystalline phase consists of stronger-shaped, ribbonlike crystallites than in the DBCH filaments.

Mechanical Properties

The results of measurements on single filaments are presented in Table VII and Figures 6 and 7. The results testify to that in chitin filaments, which occur as a result of alkaline hydrolysis of DBCH, a decrease of tensile strength σ , of elongation at rupture ε , and the initial modulus E. Such kinds of changes refer to filaments conditioned at 20% RH as well as at 65% RH. One can notice that mechanical properties of chitin filaments due to their high hygroscopicity are strongly dependent on their state of humidity. This is especially drastic in the case of elongation at rupture.

Figure 6 proves that the water content of chitin filaments very strongly influences the stress-strain curve, while for the DBCH precursor the changes are relatively small.

Table X Moisture Regain and Swelling of Chitin and DBCH Filaments

Kind of Filament	Moisture Regain at 65% RH, 20°C (%)	Swelling in Water at 20°C (%)	Swelling in Solution of Physiological Salt at 20°C (%)
DBCH	4.8	35.4	40.0
Chitin	10.9	39.8	57.9

Thermal Properties

DSC thermograms of chitin and precursor filaments are depicted in Figures 8 and 9. The thermograms show differences. In general, it may be inferred that chitin filaments exhibit greater thermal stability. The temperatures of specific thermal transitions are higher than for DBCH filaments. Thus, the first endothermic minimum, reflecting the initial stage of glass transition with reference to molecules in the amorphous phase, which are strongly entangled and are not connected with crystalline regions, appears in the case of chitin filaments at 100°C, for DBCH filaments at 80–90°C. Further, the second endothermic minimum, which can be due to the thermal decomposition of crystalline regions, starts at 330°C for chitin and at 280°C for DBCH filaments.

Electrical Properties

The ascertained results of electrical volume resistivity for chitin and precursor filaments are presented in Table VIII and Figures 10–13.

The achieved results prove that chitin fila-

ments compared to precursor DBCH filaments are characterized by a better electrical conductivity. This pertains to lower as well as to higher values of humidity.

Density and Optical Properties

Density values and the refractive indices are collected in Table IX. As one can see, there is a good correspondence between the density and light refraction ability for both kinds of filaments. The higher density of chitin filaments are fully in line with their higher degree of crystallinity.

Moisture Regain, Swelling, and Dyeability

The measured moisture regain and swelling values are presented in Table X. The stated higher values of moisture regain and swelling for chitin than for DBCH filaments can be explained by the differences in the number of hydrophilic OH groups in the absorbing water amorphous phase of both filament types. The large amount of such groups in chitin enhances the water sorption and, therefore, leads to higher swelling.

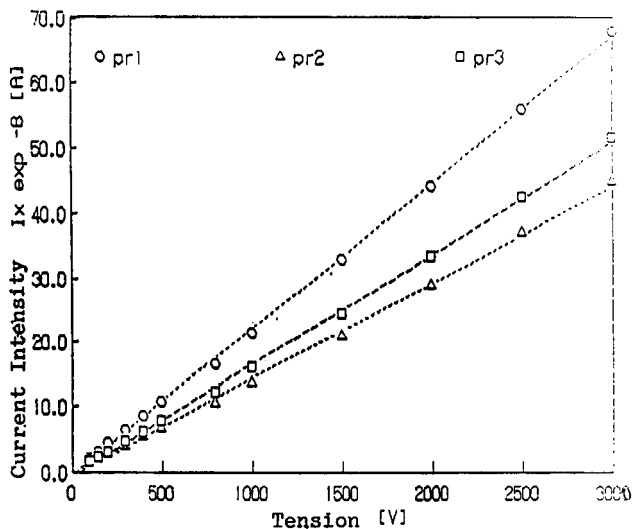


Figure 10 Electrical current intensity–tension characteristics of chitin filaments: RH = 25%; $T = 23^\circ\text{C}$.

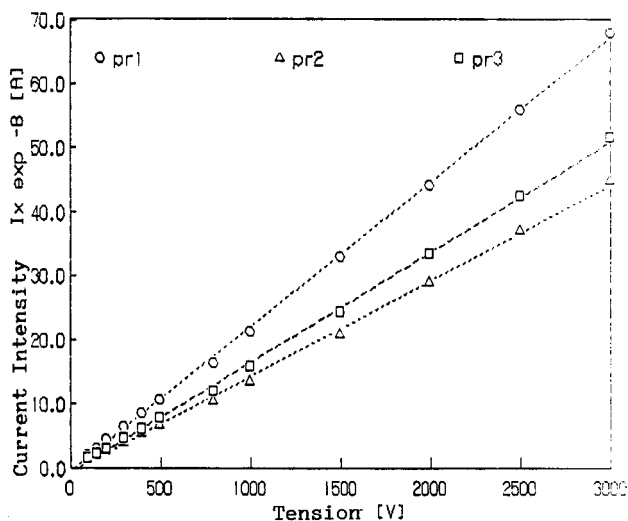


Figure 11 Electrical current intensity–tension characteristics of chitin filaments: RH = 65%; $T = 23^\circ\text{C}$.

The chitin filaments differ in respect to their dyeability from precursor DBCH filaments. They reveal a very good dyeability with direct dyestuffs and cold as well as hot reactive dyestuffs, while DBCH filaments do not exhibit such an ability. A common feature of both kinds of filaments consists of good dyeability with disperse dyestuffs.

CONCLUSIONS

1. The morphological structure of chitin filaments is characterized by very irregular shapes and developed contour line of their cross sections, by the lack of skin–core building, and by the absence of spherulitical crystalline aggregations.
2. The fine structure of chitin filaments investigated is characterized by the monoclinic lattice with unit cell $a = 4.8 \text{ \AA}$, $b = 9.83 \text{ \AA}$, $c = 10.32 \text{ \AA}$, $\gamma = 112^\circ$, and density $d_{cr} = 1.4130 \text{ g/cm}^3$; by the X-ray crystallinity degree 0.26, and lateral average crystallite sizes $D_{100} = 27.0 \text{ \AA}$, $D_{010} = 55.5 \text{ \AA}$; by the crystalline orientation factor $f_{cr} = 0.6355$. The amorphous phase is determined by density $d_{amorph.} = 1.3251 \text{ g/cm}^3$ and orientation factors

$$f_{IR1455} \text{ cm}^{-1} = 0.0137 \text{ and}$$

$$f_{IR1375} \text{ cm}^{-1} = 0.0130.$$

3. The physical properties of the chitin filaments are described by tensile strength

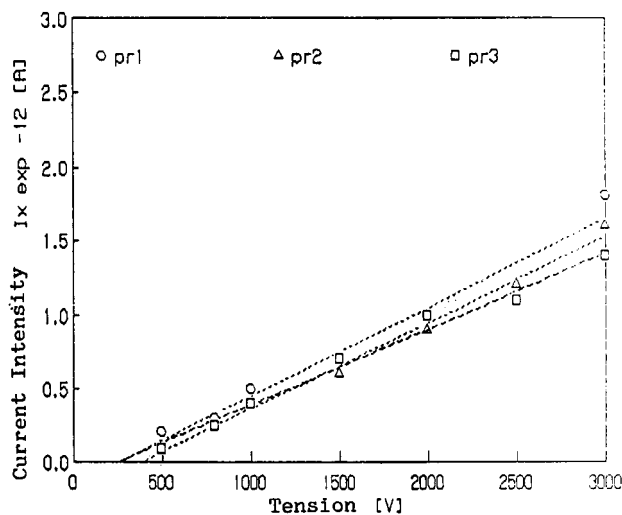


Figure 12 Electrical current intensity–tension characteristics of DBCH filaments: RH = 25%; $T = 23^\circ$.

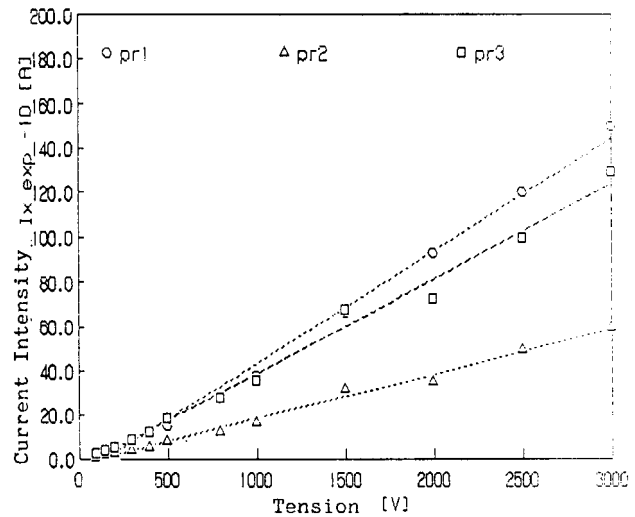


Figure 13 Electrical current intensity–tension characteristics of DBCH filaments: RH = 65%; $T = 23^\circ\text{C}$.

77.1 and 58.0 MPa, elongation at rupture 4.6 and 42.2%, initial modulus 2.2 and 1.0 GPa, correspondingly for RH = 20% and RH = 65%, by volume resistivity 1.3×10^8 and $4.8 \times 10^7 \text{ } \Omega \text{ m}$, respectively for RH = 25% and RH = 65%, by density 1.3767 g/cm^3 , by refractive index 1.5283.

4. The physicochemical properties of the chitin filaments (i.e., the swelling ability and dyeability) are as follows: swelling in water 39.8%, swelling in solution of physiological salt 57.9 %, very good dyeability by application of direct, reactive, and disperse dyestuffs.

REFERENCES

1. J. Blackwell, R. Minke, and K. A. Gardner, *Proceedings of the First Inter. Conf. on Chitin and Chitosan*, MIT Sea Grant Report 78–7,108 (1978).
2. G. Kunike, *J. Soc. Deyers Col.*, **42**, 228 (1926).
3. S. Tokura, N. Nishi, and J. Noguchi, *Polym. J.*, **11**, 781 (1979).
4. L. Szosland and G. C. East, *J. Appl. Polym. Sci.*, **58**, 2459 (1995).
5. P. H. Hermans and A. Weidinger, *J. Polym. Sci.*, **4**, 709 (1949).
6. G. Urbanczyk, *Mikrostruktura Wlokna, Badanie Struktury Krystalicznej*, WNT, Warszawa, 1988, p. 124.
7. G. Urbanczyk, *Mikrostruktura Wlokna, Badanie Orientacji Wewnetrznej*, WNT, Warszawa, 1986, p. 189.
8. R. D. B. Fraser, *J. Chem. Phys.*, **21**, 1511 (1953); **28**, 1113 (1958).

9. D. Carlstrom, *J. Biochem. Biophys. Cytol.*, **3**, 669 (1957).
10. R. Minke and J. Blackwell, *J. Mol. Biol.*, **120**, 167 (1978).
11. N. E. Dweltz, *Biochim. Biophys. Acta*, **51**, 283 (1961).
12. N. E. Dweltz, *Can. J. Chem.*, **46**, 1513 (1968).
13. J. Blackwell, K. D. Parker, and K. M. Rudal, *J. Mol. Biol.*, **28**, 383 (1967).
14. J. Blackwell, *Biopolymers*, **7**, 281 (1969).
15. K. H. Gardner and J. Blackwell, *Biopolymers*, **14**, 1581 (1975).
16. Ja. W. Genin, *Wysokomolek. Sojed.*, **26**, 2411 (1984).
17. G. L. Clark and A. F. Smith, *J. Phys. Chem.*, **40**, 869 (1936).
18. G. Urbanczyk, B. Lipp-Symonowicz, A. Jeziorny, K. Dorau, H. Wrzosek, St. Kowalska, and E. Sztajner, *Text. Res. J.*, **66**, 300 (1996).